Investigations of the carbon fibre cross-sectional areas and their non-circularities by means of laser diffraction

IOP Conf. Series: Materials Science and Engineering **942** (2020) 012034 doi:10.1088/1757-899X/942/1/012034

Investigations of the carbon fibre cross-sectional areas and their non-circularities by means of laser diffraction

Jonas J. Huether[1] **and Wilfried V. Liebig**[1]

[1]Karlsruhe Institute of Technology, Institute for Applied Materials IAM-WK, Kaiserstrasse 12, 76131 Germany

E-mail: Jonas.huether@kit.edu

Abstract. Laser diffraction is a commonly used tool to measure the fibre diameter of carbon fibres prior to mechanical testing. However, non-circularities of carbon fibres need to be considered in order to minimise measuring errors. As the work at hand demonstrates, using a single measurement of the fibre diameter may cause deviations as high as 30% from a computationally determined value. It appears that the error can be minimised by acquiring a data set of several apparent diameters as a function of the angle around the fibre axis. Based on this data, the cross-sectional area can be calculated as a circle with an averaged diameter or as an ellipse by applying an elliptical fitting procedure.

1. Introduction

Carbon fibres offer outstanding mechanical properties in relation to their low density. Thus, demand and markets for carbon fibre reinforced polymers (CFRP) are still growing and CFRP are used in various lightweight structures, for instance in the automotive, aviation and aerospace industry. However, when it comes to carbon fibre testing, the focus often lies upon composite properties rather than on single fibre testing. Nonetheless, single fibre testing is the method of choice when a better understanding of the fibre properties and how they are affected, for instance by recycling, ageing and production processes themselves, is sought.

2. State of research

Single fibre testing has its roots in the cotton industry [1–3] and several methods and measurement protocols have been transferred to technical high-modulus fibres without assuring their scientific accuracy. For instance, strains are commonly not measured on fibre scale and fibre diameters are assumed to be circular. The latter cause of error is investigated in the work at hand. Considering non-circular carbon fibre shapes is expected to allow for enhanced single fibre testing.

2.1. Carbon fibre shapes

Assuming that all types of carbon fibres are shaped perfectly circular oversimplyfies the reality. Instead, various fibre shapes co-exist in dependence of the manufacturer, the processing temperatures and other process parameters. Reviewing publications concerned with carbon

fibres, four main categories of fibre shapes emerge. The list presented here serves as a general classification and makes no claim to completeness.

a) **circular**: cross-sections of these fibres resemble a perfect circle. Exclusively for fibres of this category it is legitimate to calculate the cross-sectional area based directly on the fibre diameter [4–14].

b) **oval** and **elliptical**: fibres within this category are convex but deviate from circular shapes. Their apparent diameter varies as a function of the viewing angle [4, 14–19].

c) **kidney-shaped**: kidney-shaped fibres are, mathematically speaking, not convex. The are oval-like but possess a distinct indentation along the fibre axis [4, 6–9, 11, 14, 20–22].

d) **complex** and/or **hollow**: This category contains the largest spectrum of different fibre shapes. Published representations of fibres include trilobal, cross-like, rectangular-like and hollow (circular) fibre shapes [13, 23–31].

The four shapes are schematically presented in Figure 1 a) to Figure 1 d). A direct determination of the cross-sectional area is difficult to accomplish in tensile tests. More convenient is the measurement of an apparent fibre diameter which is then commonly used to calculate the cross-sectional area of a circle, neglecting the variety of different fibre shapes. It is evident that such a simplification is deficient for all non-circular fibres, particularly for hollow and kidney-shaped fibres as presented in Figures 1 c) and Figure 1 d).

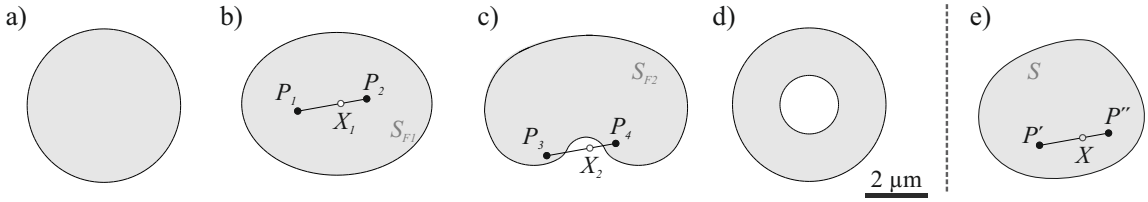

Figure 1: Categorisation of carbon fibre shapes: a) to d) are simplified shapes based on a literature review and are declared as a) circular, b) oval, c) kidney-shaped and d) complex and/or hollow. e) is a tracing of a real fibre. Shapes a), b) and e) fulfil the definition of convex sets, while c) and d) are non-convex.

The fibre shapes shown in Figure 1 a) and Figure 1 b) fulfil the definition of being convex sets, while those in Figure 1 c) and Figure 1 d) do not. With reference to Figure 1e), a set S is defined as being convex if and only if for all arbitrary points P' and P'' in S and all points X on the line segment connecting P' and P'', the points X also belong to the set S [32, 33]. If any point X does not belong to the set, the set is non-convex. Figure 1 gives an illustration with X_1 being included in the set S_{F1}, while X_2 is excluded from set S_{F2}. To apply laser diffraction techniques correctly, convexity of the fibre shape is a mandatory boundary condition.

2.2. Measurement of cross-sectional areas of carbon fibres

To obtain the cross-sectional area of carbon fibres, a range of measurement techniques exist and most of the procedures are classified in standard BS ISO-11567 [34]. In the standard it is also emphasised that the term diameter may refer to a true diameter in case of a perfectly circular fibre and to an apparent diameter when observing solely the side view of a non-circular fibre.

Laser diffraction is one technique proposed in standard BS ISO-11567 and it was first used for determining the diameters and eccentricity of metal wires [35–37] but is nowadays also applied for investigating carbon fibres. Details of the working principle of laser diffraction were published by Fedorov, Wang and Valdivia-Hernandez and Koedam [38–40], but a general explanation

shall be given in accordance with Figure 2b): Here, parallel beams of light from a laser hit the carbon fibre (i). Given the fineness of the fibre, it can be described as a single slit (ii), which is diffracting the incoming light. The resulting diffraction pattern is mathematically transformed to an apparent fibre diameter d' as a function of the angular rotation (β). If only one measurement is taken, this reading is commonly considered to calculate a circular cross-section. If a series (>2) of individual apparent diameters is measured in different angles, a circular cross-section can be computed based on an average apparent diameter. It is advisable to rotate the system in angular increments β_i, starting at 0° and completing at $(180° - \beta_i)$, to take irregular fibre shapes into consideration without giving more weight to a certain direction [11, 34, 41]. If a series of diameter readings is recorded, additional evaluation principles emerge. They are expected to be superior to the simplified circular assumption as non-circularities are considered: for instance, a procedure to approximate the carbon fibre shape by assuming an elliptical instead of a circular shape was presented by the authors in [15, 42] and is also applied in the work at hand.

Particularly, the closed measuring system LDS0200 by *CERSA-MCI* which is also incorporated in the LEX820/LDS0200 tensile tester by *Dia-Stron* is commonly used for determining diameters and/or cross-sectional areas of carbon fibres. Published examples are studies on carbon fibre tensile strength [15, 41], on the comparison between virgin and recycled carbon fibres [15, 43, 44] and on the manufacturing of carbon fibres based on cellulose/lignin precursors [45–47]. In the LEX820/LDS0200 apparatus the ends of the fibre are embedded in resin and the fibre diameter is measured once while a pretension is applied. A rocking movement of ± 8° is executed to receive an optimised laser signal. Yet, the fibre rotation and thus the rotational angle between fibre and laser source are arbitrary. The factory-set calibration of the LDS0200 is based on stainless steel wires with an uncertainty of 0.01 µm, according to the manufacturer. However, several research groups expressed doubts concerning the utilisation and calibration of laser diffraction sensors to measure carbon fibres. Particularly, the laser diffraction signal can be affected by different surfaces of the fibre [42, 48–50]. Details of standardised calibration procedures of laser diffraction sensors as well as other testing methods discussed in standard BS ISO-11567 [34] are beyond the focus of the present paper and shall neither be discussed nor used in the work at hand.

3. Experiments

All experiments were run on *Panex 35* carbon fibres manufactured by *Zoltek Toray Group*. The experiments are based on principle of laser diffraction and a computational procedure to mimic laser diffraction measurements. Both were applied to determine apparent diameters and to calculate the cross-sectional area either by assuming elliptical [15] or circular fibre shapes [34].

Figure 2a) illustrates the geometrical approach based on fibre micro sections. Two parallel tangents, $\overline{PQ}$ and $\overline{RS}$, rotated by an angle β from the horizontal axis are positioned in a manner that they coincide with the outermost curvature of the fibre section. This procedure provides an apparent diameter d as a function of the angular rotation. It mimics an experiment based on laser diffraction as shown in Figure 2b), explained in Section 2.2.

In the following, the experimental procedure based on laser diffraction and an approach based on computational geometric shapes are described. In both investigations, apparent diameters were obtained in angular steps of ($\beta_i = 10°$), from 0° to 140° in the real experiment, and from 0° to 170° in the computational approach. An angle of 140° was the maximum coverage feasible with the experimental setup described in [15] and used here.

Based on the series of individual measurements of d' as a function of the rotational angle β', a non-linear fit of least squares is run to provide the semi-major axis a and the semi-minor axis b of an approximated ellipse [15]:

$$d' = \sqrt{(2\,a\cos\beta')^2 + (2\,b\sin\beta')^2} \tag{1}$$

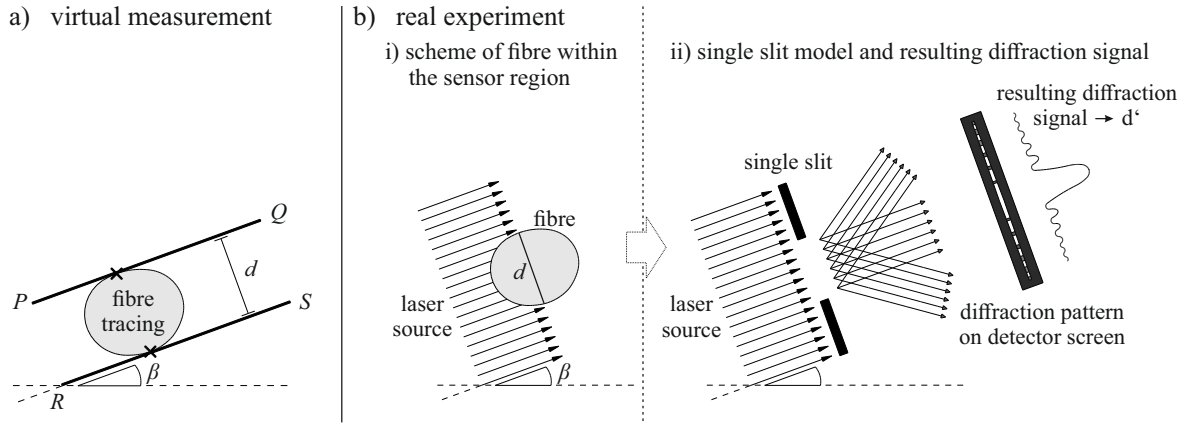

Figure 2: Laser diffraction principle: a) a set of the two parallel tangents $\overline{PQ}$ and $\overline{RS}$ imitates the measurement based on laser diffraction when the tangents touch the outermost part of a fibre tracing. b) in laser diffraction, a fibre can be seen as single slit and the occurring diffraction pattern is used to derive apparent diameters.

The geometric derivation and mathematical relationships are shown in Figure 3. With both axes, the area of the elliptical cross-section (A_{fibre}) can be calculated by:

$$A_{fibre} = \pi\, a\, b \tag{2}$$

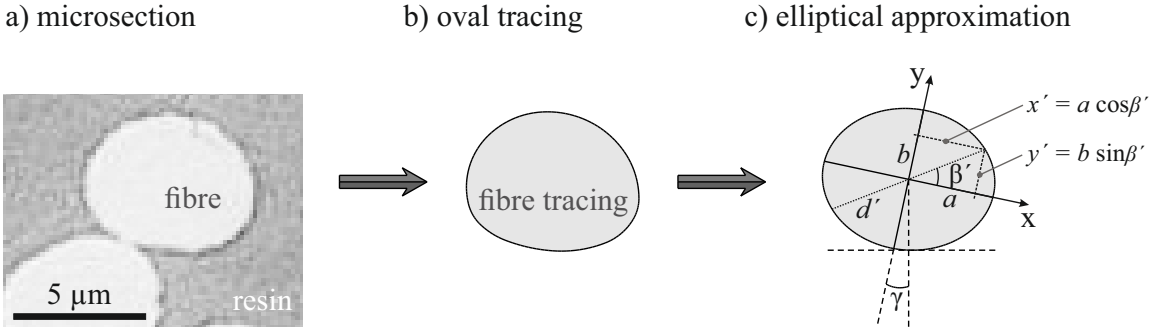

Figure 3: Elliptical approximation of an oval carbon fibre. Geometric derivation and mathematical relationships to approximate the cross-sectional area of a carbon fibre.

3.1. Laser diffraction measurements on carbon fibres

For the experimental investigations of carbon fibres, the fibres were strained and aligned with a parallel gripping system. Laser diffraction measurements were executed with the closed measuring system LDS0200. The laser diffraction sensor worked with the aforementioned factory-set calibration with steel wires. To adapt the sensor to carbon fibres, an empirically determined correction function was applied [42]: all measured apparent diameters d' were transformed to corrected diameters d'_c with Equation (3):

$$d'_c \;=\; 1.03774 \,+\, 0.96497 \cdot d' \tag{3}$$

All diameters used for the evaluations within the work at hand are corrected diameters d'_c. The laser diffraction sensor could be rotated in angular steps of 10° in respect to the fibre axis. In the investigation of real carbon fibres, no alternative procedures to verify the results could be executed, as it is impossible to evaluate the very same position along the fibre with another procedure, for instance metallographical investigations.

3.2. Computational geometric approach

To gain a database for the computational approach, fibre tracings were generated on base of microsections of ten arbitrarily chosen carbon fibres, shown in ascending cross-sectional area as geometric shape 1 to 10 in Figure 4. For these shapes, the 0°-direction is arbitrarily chosen and exemplary shown for fibre 1.

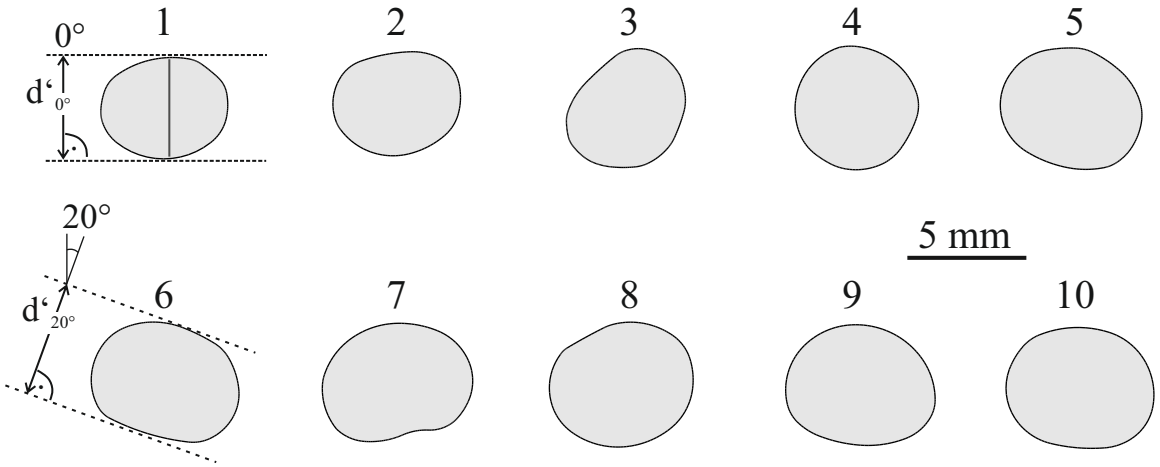

Figure 4: Ten fibre tracings sorted by ascending cross-sectional area.

Apparent diameters were determined as follows: the *true* cross-sectional area was determined computationally by image analysis to serve as comparison. A set of two parallel tangents was positioned in a way that they coincided with the outermost curves of the shape, starting at an initial angle of 0°. The tangents were then rotated in steps of 10°, providing a series of apparent diameters as a function of the angle. For each shape, 18 measurements were taken from $d'_{0°}$ to $d'_{170°}$ to fully cover the geometric shape. 18 measurements were the database for different procedures to calculate the cross-sectional area of each fibre tracing.

3.3. Nomenclature of different calculation procedures

The following calculations were used:

- **ellipse 140** was calculated by an elliptical fit according to [15]. Apparent diameters were taken in steps of 10° from 0° to 140°. This corresponds to the constraints caused by the experimental setup used in the work at hand for tensile tests on fibres.
- **ellipse 170** is analogous to procedure *ellipse 140* but angles up to 170° were considered. This corresponds to a half circle, which is sufficient to cover the complete shape by the fitting procedure. This calculation was solely feasible for the computational approach.
- **circle random**, **circle random 0** and **circle random 40** connote that one apparent diameter for each fibre tracing was randomly picked to calculate its circular cross-sectional area. Fortuitousness was ensured by the fact that the fibres were not specifically angled before mechanical testing or metallographic investigation.

- **circle max** and **circle min** signify that the maximum or the minimum apparent diameter of each fibre tracing were used to calculate a circular cross-sectional area.
- **circle 0/60/120** connotes that three apparent diameters were averaged to calculate a circular cross-sectional area, with the 0° - direction being the starting point and then rotating the set of tangents by 60°.
- **circle 0-140** was calculated by averaging the same apparent diameters as for *ellipse 140* but instead of using the described elliptical fit, 15 apparent diameters were used to calculate a circular area.

4. Results

In the following, results of the experimental and computational approach are presented.

4.1. Laser diffraction

200 carbon fibres were measured with the laser diffraction sensor according to the procedure detailed in Section 3.1. Based on 15 apparent diameters per fibre, cross-sectional areas were calculated with either the elliptical approach or based on circular assumptions. Results are plotted in Figure 5: Figure 5 a) displays the complete data set, Figure 5 b) highlights the interval from fibre number 85 to 115. The dashed lines are the envelope curve obtained by calculating the circular area based on the maximum or minimum apparent diameter, respectively.

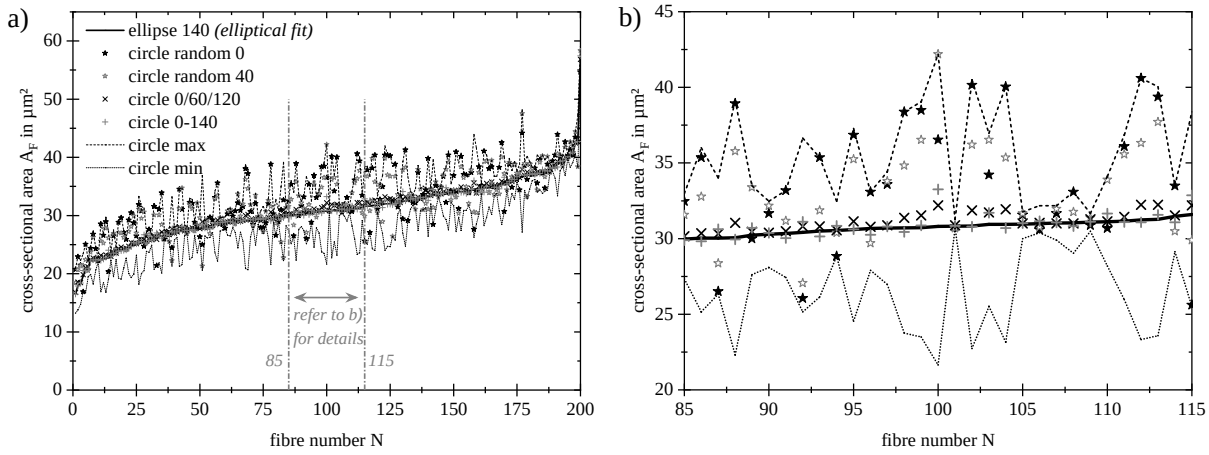

Figure 5: a) Cross-sectional areas of 200 fibres were determined based on different calculations. The dataset is sorted by ascending cross-sectional area of the elliptical fitting procedure (ellipse 140). For each fibre number N, the differently calculated results are plotted. b) For better clarity, the segment between fibre number 85 and 115 is shown enlarged.

4.2. Computational approach

Ten fibre tracings were measured according to the procedure presented in Section 3.2. Based on 18 individual apparent diameters per fibre tracing, the cross-sectional areas were calculated in different ways. Results are plotted versus the computational (*true*) value in Figure 6 a). In addition, Figure 6 b) displays the calculations for each fibre tracing, analogously to Figure 5 b). As Figure 6 a) highlights, all procedures depicted there tend to overestimate the cross-sectional area.

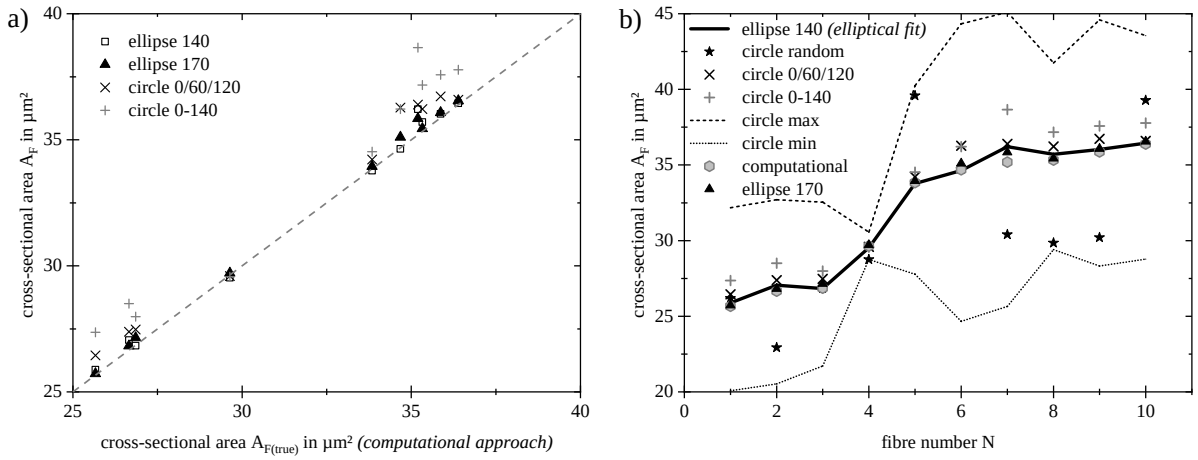

Figure 6: a) Cross-sectional areas calculated based on different procedures plotted versus the cross-sectional area determined computational (*true* value). b) Different calculation approaches for each fibre tracing; illustrated analogous to Figure 5 b).

5. Discussion

The work at hand has its focus on evaluating to what extend laser diffraction sensors provide reliable measurements of the cross-sectional area of carbon fibres. Laser diffraction is a widely used principle to determine the cross-sectional areas of carbon fibres. However, only few publications considered the non-circularity of fibre shapes, by either recording and averaging a series of individual apparent diameters in various rotational angles to increase the statistical certainty [11, 41] or by hypothesizing elliptical shapes [15, 42].

In Section 4 it was shown that calculations of the cross-sectional area of irregularly shaped carbon fibres vary significantly depending on whether circular or oval shapes are assumed, for both, the experimental measurements on carbon fibres and the computational approach on fibre sections.

This effect shall be further described in accordance with Figure 7. The value equivalence line represents the values obtained by the elliptical fitting procedure based on 15 apparent diameters (*ellipse 140*) for both, the experimental and the computational approach. Procedure *ellipse 140* was chosen for comparative purposes, as its values are available in both, the experimental and the computational approach. Here, cross-sectional areas calculated based on the circular assumptions are plotted as small symbols for the experimental approach (200 fibres) and as large symbols for the computational approach (10 fibre tracings, shown in Figure 4). Again it becomes obvious that a cross-sectional area based on one (randomly picked) apparent diameter causes large deviations from the elliptical fitting procedure. As shown in Figure 6 b), values obtained by the elliptical fitting procedures differ only slightly from the *true* values determined computationally. Moreover, data in Figure 7 indicates that circular calculations based on laser diffraction measurements tend to overestimate the cross-sectional area: linear fits of the experimental data are shifted towards larger values compared to the value equivalence line. This effect is most prominent for the randomly picked apparent diameters. Listed in Table 1 are the slope, the intersection with the axis of ordinates and the Pearson correlation coefficient. The correlation coefficient and the slope for the linear fits of *circle 0/60/120* and *circle 0-140* are close to unity, and the deviation from the origin is low (0.5 and 0.1, respectively). When picking a single random value (*circle random*), the correlation is rather low (0.811) and slope and origin deviate significantly from unity. In general, the overestimation caused by laser diffraction measurements can be explained by the fact that crenellations and indentations along the fibre

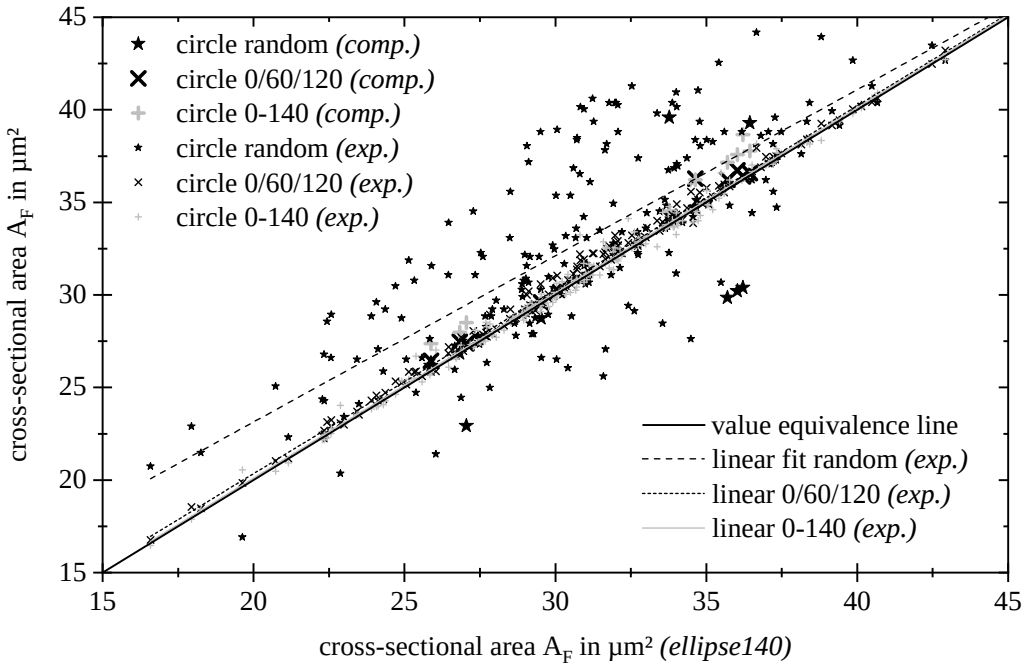

Figure 7: Calculations of circular cross-sectional areas of carbon fibres and their tracing compared to the elliptical fitting procedure. Computational investigations of fibre tracings are labelled *(comp.)*, experimental measurements on carbon fibres *(exp.)*. Procedure *ellipse 140* serves as comparison as it was available for both, the experimental and the computational approach.

cannot be detected by the laser. This effect is expected for both, the circular and the elliptical assumption. However, it tends to be more prominent when assuming circular shapes, a trend depicted in Figure 6 b) where all computational values (obtained by image analysis) are below the circular assumptions *circle 0/60/120* and *circle 0-140* and the elliptical procedures *ellipse 140* and *ellipse 170*.

Table 1: Evaluation of the linear fits of experimental data in Figure 7.

	circle random	circle 0/60/120	circle 0-140
slope	0.898	0.994	1.001
intersection with axis of ordinates in µm^2	5.2	0.5	0.1
Pearson correlation coefficient	0.811	0.998	0.996

The deviation from the elliptical fit shall be further discussed for the experimental results on 200 carbon fibres: relative deviations between elliptical and circular assumptions were as high as 38 %. Both, *circle 0-140* and *circle 0/60/120* show mostly deviations below 4 %, with the former showing some deviations higher than 4 % compared to the values obtained by the elliptical fit. Opposed to that, picking a random or the maximum apparent diameter to calculate a circular cross-sectional area yields a wide range of deviations up to more than 30 %. For the randomly picked apparent diameters, half of the data set (100 fibres) deviates 7 % or more in cross-sectional area, for the maximum apparent diameters 100 fibres deviate 10 % or more. As elucidated, laser diffraction is a common tool to investigate the cross-sectional area of carbon

fibres [11, 15, 41–47]. The data provided in the work at hand clearly indicates that when applying laser diffraction, picking a single apparent diameter might cause significant measuring errors. Instead, it is recommended to use a series of individual measurements in equidistant angular steps and an averaged diameter to calculate the cross-sectional area. Considering non-circular shapes by applying an elliptical fitting procedure proved to be a purposeful approach, as this procedure is more suitable when the laser diffraction sensor cannot be rotated completely around the fibre axis [15, 42]. Without detailed quantification, some additional aspects that might decrease the quality and reliability of determining the cross-sectional area by means of laser diffractometry shall be listed, partly in accordance with Figure 8. These effects can occur separately or collectively. The likelihood and severity of erroneous readings is expected to rise from a) to e). If the fibres exhibit perfect circular shapes (a), the limiting factor is the accuracy of the laser diffraction sensor. As shown in the work at hand, oval shapes (b) demand for recording a series of individual diameter measurements [15, 42]. Kidney-shaped fibres (c: [4, 6–9, 11, 14, 20–22]), which do not fulfil the definition of being convex sets, will affect the measurement as the size of undercuts cannot be detected by laser diffraction. Crenellations along the fibre (d) are an additional deviation from the convex shape and the cross-sectional area will be overrated. Debris like dust (e) may also interfere with the laser beam and deteriorate the measurement. Not shown graphically but nonetheless relevant sources of inaccuracies are listed at what follows: misalignments between the laser beam and the fibre may influence the measurement. Furthermore, laser diffraction sensors average the apparent diameter along a certain increment of the fibre, for instance approximately 2 mm in case of the LDS0200. According to the manufacturer, *Diastron*, this device has a resolution of 0.01 µm which is another limiting factor of the measurement accuracy. The device is calibrated with steel wires, and as explained earlier, the calibration needs to be adjusted to carbon fibres [42].

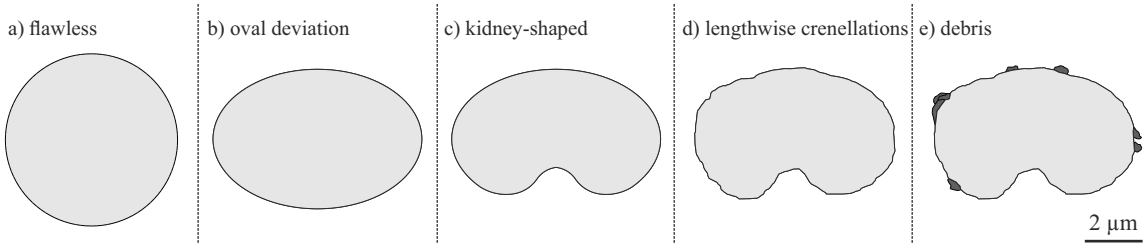

Figure 8: Effects on the quality of laser diffraction measurements: the more irregular the fibre shape and the higher the amount of undercuts and debris, the lower the quality of laser diffraction measurements.

6. Conclusion

It can be concluded that when applying laser diffraction techniques to determine the diameter of carbon fibres, the non-circularity of carbon fibres should be considered. Firstly, the fibre population should be investigated microscopically to detect the predominant fibre shape. Secondly, a series of apparent diameters can be averaged to increase statistical certainty. Here, the measuring sensor has to be rotated at constant angular steps in relation to the fibre, while ensuring that none direction is given more weight to. Thirdly, calculations of cross-sectional areas can be improved by considering oval or elliptical shapes instead of circular fibre shapes.

7. Acknowledgement

The authors would like to thank Michael Seitz for his scientific contribution to this article.

References

[1] 2012 *ASTM standard D1445/D1445M – 12: Standard Test Method for Breaking Strength and Elongation of Cotton Fibers (Flat Bundle Method)* (West Conshohocken, PA)

[2] Osumi G and Kato E 1937 *Journal of the Textile Institute Transactions* **28** T129–T144 ISSN 1944-7027

[3] Pressley E H 1942 *American Society for Testing and Materials Bulletin* **118** 13–17

[4] Naito K, Tanaka Y, Yang J M and Kagawa Y 2008 *Carbon* **46** 189–195 ISSN 00086223

[5] Naito K, Yang J M, Tanaka Y and Kagawa Y 2012 *Journal of Materials Science* **47** 632–642 ISSN 0022-2461

[6] Naito K, Tanaka Y and Yang J M 2017 *Carbon* **118** 168–183 ISSN 00086223

[7] Kumar S, Anderson D P and Crasto A S 1993 *Journal of Materials Science* **28** 423–439 ISSN 0022-2461

[8] Endo M 1988 *Journal of Materials Science* **23** 598–605

[9] JDH Hughes 1986 *Carbon* **24** 551–556 ISSN 00086223

[10] Cho T, Lee Y S, Rao R, Rao A M, Edie D D and Ogale A A 2003 *Carbon* **41** 1419–1424 ISSN 00086223

[11] Tzeng S S and Chang F Y 2001 *Materials Science and Engineering: A* **302** 258–267 ISSN 09215093

[12] Vezie D L and Adams W W 1990 *Journal of Materials Science Letters* **9** 883–887 ISSN 0261-8028

[13] Liu X, Wang R, Wu Z and Liu W 2012 *Materials Letters* **73** 21–23 ISSN 0167577X

[14] Kobets L P and Deev I S 1998 *Composites Science and Technology* **57** 1571–1580 ISSN 02663538

[15] Huether J, Esse D, Rupp P, Seitz M and Weidenmann K 2019 *Measurement Science and Technology* **30** 1–12 ISSN 0957-0233

[16] Saburow O, Huether J, Maertens R, Trauth A, Kechaou Y, Henning F and Weidenmann K A 2017 *Procedia CIRP* **66** 265–270 ISSN 22128271

[17] Li Z, Zhang D, Qin W and Geng D 2017 *Proceedings of the Institution of Mechanical Engineers, Part B: Journal of Engineering Manufacture* **231** 2347–2358 ISSN 0954-4054

[18] Paris O, Loidl D, Müller M, Lichtenegger H and Peterlik H 2001 *Journal of Applied Crystallography* **34** 473–479 ISSN 0021-8898

[19] Fitzer E 1989 *Carbon* **27** 621–645 ISSN 00086223

[20] Daumit G and Ko Y 1986 *High tech: The way into the nineties – Proceedings of the 7th International Conference of the Society for the Advancement of Material and Process Engineering European Chapter* **7** 201–213

[21] Marcuzzo J, Otani C, Polidoro H and Otani S 2013 *Materials Research* **16** 137–144 ISSN 0033-4545

[22] Johnson J W and Thorne D J 1969 *Carbon* **7** 659–661 ISSN 00086223

[23] Curtis P T and Travis S 1999 *Plastics, Rubber and Composites* **28** 201–209 ISSN 1465-8011

[24] Liu Y, Chae H, Choi Y and Kumar S 2015 *Journal of Materials Science* **50** 3614–3621 ISSN 0022-2461

[25] Wang C Y, Li M W, Wu Y L and Guo C T 1998 *Carbon* **36** 1749–1754 ISSN 00086223

[26] Xie W, Cheng H, Chu Z, Chen Z and Long C 2011 *Ceramics International* **37** 1947–1951 ISSN 02728842

[27] Park S J, Seo M K, Shim H B and Rhee K Y 2004 *Materials Science and Engineering: A* **366** 348–355 ISSN 09215093

[28] Gulgunje P, Newcomb B, Gupta K, Chae H, Tsotsis T and Kumar S 2015 *Carbon* **95** 710–714 ISSN 00086223

[29] Hunt M, Saito T, Brown R, Kumbhar A and Naskar A 2012 *Advanced materials (Deerfield Beach, Fla.)* **24** 2386–2389

[30] McMahon P E 1973 Graphite fiber tensile property evaluation *Analysis of the Test Methods for High Modulus Fibers and Composites* ed Whitney J M (West Conshohocken, PA: ASTM International) pp 367–367–23

[31] Eom S Y and Ryu S K 2010 *Korean Journal of Chemical Engineering* **27** 1592–1595 ISSN 0256-1115

[32] Bonnesen T and Fenchel W 1934 *Theorie der konvexen Körper* (Berlin, Heidelberg: Springer) ISBN 9783540062349

[33] Schneider R 1993 *Convex bodies: The Brunn-Minkowski theory* (*Encyclopedia of mathematics and its applications* vol 44) (Cambridge and New York: Cambridge University Press) ISBN 9780521352208

[34] British Standards 2018 BS-ISO 11567:2018: Carbon fibre - Determination of filament diameter and cross-sectional area: Carbon materials

[35] Blohm W, Sikora H and Beining A 1999 Durchmessermessung mit Beugungssäumen sowie elektronische Verschmutzungskorrektur - European Patent Office - EP 0924493 B1: Europäische Patentschrift

[36] Khodier S 2004 *Optics & Laser Technology* **36** 63–67 ISSN 00303992

[37] Troll J and Baker C 1972 US Patent 3659950A – Laser apparatus for detecting the size and form of filamentary material by measuring diffracted light

[38] Fedorov M E 2015 *IOP Conf. Ser.: Mater. Sci. Eng.* **81** 1–10 ISSN 1757-8981

[39] Wang H and Valdivia-Hernandez R 1995 *Measurement Science and Technology* **6** 452–457 ISSN 0957-0233

[40] Koedam M 1966 *Philips technical review* **27** 208–211

[41] Islam F, Joannès S, Bucknell S, Leray Y, Bunsell A and Laiarinandrasana L 2020 *Journal of reinforced plastics and composites* **39** 144–162

[42] Huether J 2020 - in print *Disseration, Schriftenreihe des Instituts für Angewandte Materialien, Band 84*

[43] Pickering S J, Turner T A, Meng F, Morris C N, Heil J P, Wong K H and Melendi-Espina S 2015 Developments in the fluidised bed process for fibre recovery from thermoset composites *2nd Annual Composites and Advanced Materials Expo, CAMX 2015; Dallas Convention CenterDallas; United States* pp 2384–2394

[44] Fischer H and Schmid H 2013 *Kunststoffe* **103** 88–91

[45] Kleinhans H and Salmén L 2016 *Journal of Applied Polymer Science* **133** 119 ISSN 0021-8995

[46] Nowak A, Hagberg J, Leijonmarck S, Schweinebarth H, Baker D, Uhlin A, Tomani P and Lindbergh G 2018 *Holzforschung* **72** 81–90

[47] Bengtsson A, Bengtsson J, Olsson C, Sedin M, Jedvert K, Theliander H and Sjöholm E 2018 *Holzforschung* **72** 1007–1016

[48] Li C T and Tietz J 1990 *Journal of Materials Science* **25** 4694–4698 ISSN 0022-2461

[49] Meretz S, Linke T, Schulz E, Hampe A and Hentschel M 1992 *Journal of Materials Science Letters* **11** 1471–1472 ISSN 0261-8028

[50] Perry A, Ineichen B and Eliasson B 1974 *Journal of Materials Science* **9** 1376–1378